

## CHANNEL ESTIMATION ALGORITHMS COMPARISON FOR MULTIBAND-OFDM

Raffaello Tesi, Matti Hämäläinen, Jari Iinatti  
Centre for Wireless Communications  
P.O.Box 4500, FI-90014 University of Oulu, FINLAND

### ABSTRACT

This paper studies the effects of channel estimation in ultra wideband (UWB) systems using a multiband-OFDM (MB-OFDM) approach. The system used consists of a three-band OFDM transmitter, each band having 128 equally spaced sub-carriers, which carry both the information data and the pilot signals. The channel estimation is based on the principle of pilot-symbol aided channel estimation (PACE), and it has been implemented using comb-type and block-type pilot sub-carrier arrangements. The algorithms used here are based on the least squares (LS) and the linear minimum mean-square error (LMMSE) approaches supported by linear and cubic interpolation, and an IFFT-based time channel estimation, which uses a zero-padding interpolation approach with and without Wiener filtering. In frequency domain algorithms, phase compensation is also taken into account. Bit error rate (BER) versus signal-to-noise ratio  $E_b/N_0$  results show that the frequency based methods generally perform better than the corresponding time based ones. Furthermore, the performances of LS and LMMSE methods are quite similar, leading us to suggest the use of LS estimator for uncoded MB-OFDM systems. Phase compensation is required in comb-type pilot sub-carrier arrangement when a low number of pilot sub-carriers is used.

### I INTRODUCTION

Orthogonal frequency division multiplexing (OFDM) is one of the solutions taken into account when implementing MB-UWB systems [1–4]. The two main reasons are the simplicity and reliability; Simplicity of implementation, since MB-OFDM can be seen as an extension of the present OFDM standard for wireless LANs [5], and reliability since it uses a well-proved technology in an ultra wideband context. If compared with a single-band impulse radio (IR), the MB approach optimises the use of UWB spectrum allocation. Its drawback is the requirement of signal generators that are able to switch quickly between succeeding frequencies [3].

The multiband OFDM approach is transmitting OFDM symbols alternatively in different bands. Each band consists of 128 equally spaced sub-carriers occupying a bandwidth of 528 MHz. Thus, the spacing between two consecutive sub-carriers is 4.125 MHz [1]. The frequency of operation for Mode 1 (mandatory mode) devices consists of transmitting symbols on three different bands placed in the lower part of the entire 3.1-

10.6 GHz band, thus having a total bandwidth occupation of approximately 1.6 GHz (see Figure 1).

The IEEE-adopted modified Saleh-Valenzuela (SV) model [6] has been used throughout this study as a channel reference. In this model, multipath components arrive in clusters and within one pulse duration, so intra-pulse interference is also present.

The main reference for channel estimation in MB-OFDM is the proposal for IEEE [1], since the further literature seems very poor on this subject. The reliability of the existing channel estimation algorithms in an UWB environment is an important issue, due to the different channel response, if compared UWB to the standard wideband transmission [7]. The modified SV-model in a MB-OFDM environment shows similarities with a “fast” Rayleigh fading channel with additional shadowing [8]. As pointed out in [9], MB-OFDM system has also been seen more sensitive to imperfect channel estimation than the corresponding singleband direct sequence based UWB system (DS-UWB). In [9], a least square channel estimation method was applied for MB-OFDM system, whereas DS-UWB was exploited with a sliding correlator approach.

In this paper, a comparative performance study of several existing channel estimation algorithms applied to the MB-OFDM system are given. Due to the typical spectral characteristics of the OFDM transmission, these methods have been implemented in the frequency domain, although a passage to the time domain is done when the estimated pilots are interpolated. Two types of pilot channel assignments have been considered: a comb-type pilot sub-carrier arrangement, where the pilots are transmitted within each symbol, and a block-type arrangement, where a symbol containing only channel pilots is transmitted within a certain time interval. The implemented channel algorithms are based on least squares (LS), linear minimum mean-squared error (LMMSE), and FFT algorithms. In the first two cases, linear and cubic interpolations have been applied to reconstruct the entire channel in the comb-type pilot sub-carrier arrangement.

The paper is structured as follows. An overview of the MB-OFDM technique is given in the second section. The third section explains the channel estimation algorithms used. In the fourth section, the simulation results will be shown and discussed. Finally, in the fifth section, the paper is concluded and further work directions are pointed out.

## II SYSTEM MODEL

### A. MB-OFDM system

The main difference of MB-OFDM transmission compared to the existing OFDM techniques [5] is that, in MB case, the total allocated spectrum  $B_{\text{tot}}$  is divided into  $N_b$  subbands. Each band is composed by  $N_c = 128$  sub-carriers where a single OFDM symbol is stuffed. The transmission sequence is then composed by a succession of symbols placed in different bands, so the total bandwidth occupation equals  $B_{\text{tot}}$ . An idea of the bandwidth allocation is given in Fig. 1 [1]. The peculiarities of MB-OFDM are summarized in Table 1.

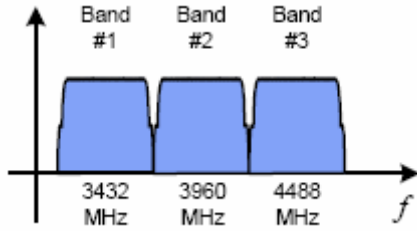


Figure 1. MB-OFDM band allocation for Model 1 devices.

Table 1. MB-OFDM specification parameters.

Parameter	Value
Modulation	QPSK
Number of bands in Mode 1	3
Number of sub-carriers	$128 \times 3 = 384$
Centre frequency of each band	3.43, 3.96, 4.49 GHz
Bandwidth of each band	528 MHz
Sub-carrier frequency spacing	4.125 MHz
Channel bit rate	640 Mbps

### B. Modified Saleh-Valenzuela Channel Model

The UWB system performance is studied using the modified Saleh-Valenzuela channel models [6], which are adopted by the IEEE802.15.3a study group as reference models for high data rate UWB system studies. SV-models are not based on the UWB channel soundings, but have been selected as the first reference models. In this study, the first (SV1) out of totally four defined SV-models has been utilized to describe the line-of-sight (LOS) channel within 0 – 4 m [6] where the high rate UWB links would be exploited at first.

Since the OFDM system is defined in frequency domain, also the channel has been modeled by calculating the Fourier transform of the time domain channel impulse response, which leads to [8]

$$C(f) = \sum_{l \geq 0} \sum_{k \geq 0} \alpha_{k,l} \exp(-j2\pi f(T_l + \tau_{k,l})), \quad (1)$$

where  $T_l$  is the delay of the  $l$ -th cluster,  $\alpha_{k,l}$  and  $\tau_{k,l}$  represent the gain and the delay of the  $k$ -th ray of the  $l$ -th cluster, respectively. For more details about the SV-channel models, please refer to [6].

### C. Channel Estimation Techniques

The techniques studied here are all based on the principle of pilot-symbol aided channel estimation (PACE) [10]. The pilot symbols have been inserted into the signal with two different approaches, as shown in Figure 2 [11]. In a block-type (BT) pilot sub-carrier arrangement, the pilots compose a full OFDM symbol, which is transmitted regularly after a fixed number of data symbols,  $N_D$ . In a comb-type (CT) pilot sub-carrier arrangement, the pilots are interleaved with the data within each OFDM symbol. In the latter case, interpolation is required in order to estimate the channel over all the sub-carriers.

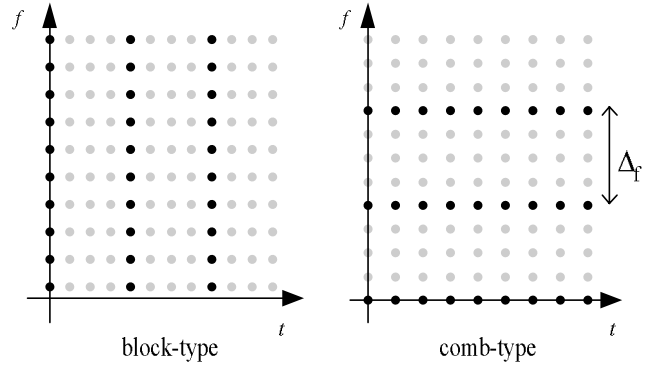


Figure 2. Possible allocation of the pilot sub-carriers.

#### 1) Frequency domain algorithms

Let us assume that a number of pilot symbols,  $N_p$ , is interleaved in  $N_c$  sub-carriers composing an OFDM symbol with a fixed frequency-spacing  $\Delta_f$ . Following the notation from [12], the received signal  $\mathbf{Y}$  characterizing one OFDM symbol can be written as

$$\mathbf{Y} = \mathbf{X}\mathbf{H} + \mathbf{N}, \quad (2)$$

where  $\mathbf{X} = \text{diag}(X_0, \dots, X_{N_c-1}) \in \mathbb{C}^{N_c \times N_c}$  is the transmitted symbol. The channel transfer function is presented as  $\mathbf{H} = [H_0, \dots, H_{N_c-1}]^T \in \mathbb{C}^{N_c \times 1}$  and the additive white Gaussian noise (AWGN) as  $\mathbf{N} = [N_0, \dots, N_{N_c-1}]^T \in \mathbb{C}^{N_c \times 1}$ , respectively. Then the transmitted signal sequence that is containing only pilots can be written as  $\tilde{\mathbf{X}} = \{\tilde{X}_{\tilde{i}}\} = \{X_i\}$ , with  $i = \tilde{i}\Delta_f$ . In the same way, we can define  $\tilde{\mathbf{H}}$  and  $\tilde{\mathbf{N}}$  so that the received OFDM signal that contains only the pilot symbols is

$$\tilde{\mathbf{Y}} = \tilde{\mathbf{X}}\tilde{\mathbf{H}} + \tilde{\mathbf{N}}. \quad (3)$$

We also assume that  $|X_i| = 1 \forall i$ .

The first studied channel estimation algorithm goes under the name of least squares (LS). It provides the first estimate of the channel transfer function by dividing the received signal by the pilot-symbol sent, such as

$$\tilde{\mathbf{H}}_{\text{LS}} = \tilde{\mathbf{X}}^H \tilde{\mathbf{Y}} = \tilde{\mathbf{H}} + \tilde{\mathbf{X}}^H \tilde{\mathbf{N}}, \quad (4)$$

with  $\tilde{\mathbf{X}}^H \tilde{\mathbf{X}} = \mathbf{I}$ .

The second studied scheme is based on linear minimum mean-squared error (LMMSE), and it is based on the knowl-

edge of the auto-correlation matrix of the channel frequency response, defined as [11]

$$\mathbf{R}_{\tilde{\mathbf{H}}\tilde{\mathbf{H}}} = \mathbb{E}\{\tilde{\mathbf{H}}\tilde{\mathbf{H}}^H\}. \quad (5)$$

Then, the estimated channel can be written as [11]

$$\tilde{\mathbf{H}}_{\text{LMMSE}} = \mathbf{R}_{\tilde{\mathbf{H}}\tilde{\mathbf{H}}} \left( \mathbf{R}_{\tilde{\mathbf{H}}\tilde{\mathbf{H}}} + \sigma_n^2 (\tilde{\mathbf{X}}\tilde{\mathbf{X}}^H)^{-1} \right)^{-1} \tilde{\mathbf{H}}_{\text{LS}}, \quad (6)$$

where  $\sigma_n^2$  represents the noise variance. Due to a further simplification [11,13], (6) can be rewritten as

$$\tilde{\mathbf{H}}_{\text{LMMSE}} = \underbrace{\mathbf{R}_{\tilde{\mathbf{H}}\tilde{\mathbf{H}}} \left( \mathbf{R}_{\tilde{\mathbf{H}}\tilde{\mathbf{H}}} + \left( \frac{E_b}{N_0} \right)^{-1} \mathbf{I} \right)^{-1}}_{\mathbf{Z}} \tilde{\mathbf{H}}_{\text{LS}}. \quad (7)$$

In our case, we will consider that the auto-correlation matrix and  $E_b/N_0$  are known a priori, so that  $\mathbf{Z}$  needs to be calculated only once.

In the both approaches explained above, interpolation must be done in order to estimate the channel for the data sub-carriers. Two interpolation methods have been considered here. The notation used in the following will be related to the LS case, but also the LMMSE can be treated with the same approach.

In linear estimation, two successive pilot sub-carriers are used to determine the channel response for the sub-carriers located in the middle. Analytically, the  $k$ -th sub-carrier will be calculated as [11]

$$\hat{H}(k) = \hat{H}(m\Delta_f + l) = \tilde{H}_{\text{LS}}(m) + \frac{l}{\Delta_f} (\tilde{H}_{\text{LS}}(m+1) - \tilde{H}_{\text{LS}}(m)), \quad 0 \leq l < \Delta_f, \quad (8)$$

where  $m\Delta_f < k < (m+1)\Delta_f$  and  $m = 0, \dots, N_p - 1$ .

The second-order polynomial interpolation can be expressed as [11]

$$\hat{H}(k) = \hat{H}(m\Delta_f + l) = C_1 \tilde{H}_{\text{LS}}(m+1) + C_0 \tilde{H}_{\text{LS}}(m) + C_{-1} \tilde{H}_{\text{LS}}(m-1), \quad (9)$$

where

$$\begin{cases} C_1 = \frac{\alpha(\alpha+1)}{2} \\ C_0 = -(\alpha-1)(\alpha+1) \\ C_{-1} = \frac{\alpha(\alpha-1)}{2}, \end{cases} \quad (10)$$

and  $\alpha = l // N_c$ , while  $k$  and  $m$  are defined as for (8).

### 2) Time domain algorithms

A different approach used for channel estimation is the time domain algorithm (TD). This method is actually another way of performing the interpolation of the LS estimate using two successive DFTs and zero padding. The drawback of this approach is the leakage effect observed when performing the

IDFT having a finite number of inputs, which will give poorer results than the frequency domain algorithms. Denoting with  $\tilde{\mathbf{F}}$  the  $N_p$ -point DFT matrix, the LS channel estimate  $\tilde{\mathbf{H}}_{\text{LS}}$  is transformed into the time domain as follows [12]

$$\hat{\mathbf{H}}_{\text{ZP}} = \tilde{\mathbf{g}}_{\text{LS}} = \frac{1}{N_p} \tilde{\mathbf{F}}^H \tilde{\mathbf{H}}_{\text{LS}}. \quad (11)$$

Calling  $\hat{\mathbf{g}}_{\text{ZP}}$  the vector obtained by zero-padding  $\tilde{\mathbf{g}}_{\text{LS}}$  with  $N_c - N_p$  zeros, the DFT-based interpolation is then performed as

$$\hat{\mathbf{H}}_{\text{ZP}} = \mathbf{F} \mathbf{I}_{N_c \times N_p} \hat{\mathbf{g}}_{\text{ZP}}, \quad (12)$$

where  $\mathbf{F}$  is the  $N_c$ -point DFT matrix, and  $\mathbf{I}_{N_c \times N_p}$  represents the  $N_p \times N_c$  identity matrix.

In order to smooth the output of the interpolator, the use of Wiener filter can be adopted. This approach requires the knowledge of the channel impulse response similarly with LMMSE case. In this case, instead of zero-padding, the estimate of the time channel response is calculated as [12]

$$\hat{\mathbf{g}}_{\text{WF}} = \mathbf{w} \tilde{\mathbf{g}}_{\text{LS}}, \quad (13)$$

where  $\mathbf{w} = \tilde{\mathbf{F}}^H \mathbf{R}_{\tilde{\mathbf{H}}\tilde{\mathbf{H}}}^{-1} \tilde{\mathbf{F}} \mathbf{R}_{\tilde{\mathbf{g}}_{\text{LS}}\tilde{\mathbf{g}}_{\text{LS}}}$ .

### 3) Phase recovery

A supplementary error in channel estimation is related to phase recovery errors. This error comes from a group delay of the received OFDM signal before demultiplexing, which has high impact on linear interpolation, and consequently causes higher distortion to the estimated channel in comb-type systems. Our study will not take into account the presence of inter-symbol interference. A simplified method of phase recovery can be applied to linear and polynomial interpolators since they are not sensitive to frame position error when the frame offset is small, and it can be expressed as [11]

$$\tilde{\theta}_p = \angle \frac{1}{N_c - 1} \sum_{m=0}^{N_p-2} \tilde{H}_{\text{LS}}^*(m) \tilde{H}_{\text{LS}}(m+1). \quad (14)$$

This value can then be used to pre-compensate the LS estimation as

$$\tilde{H}_{\text{LS,pe}}(m) = \tilde{H}_{\text{LS}}(m) \exp(j\tilde{\theta}_p m), \quad (15)$$

where ‘‘pe’’ denotes the phase estimation. After this, LMMSE estimation is performed and interpolated, and then the phase is restored by multiplying the output by  $\exp(-j\tilde{\theta}_p m)$ .

## III SIMULATION RESULTS

The simulations carried out for this study consider the following estimation approaches: LS with TD, LS with TD and Wiener filtering, LS and LMMSE with linear and cubic interpolation, LS and LMMSE with linear interpolation and phase compensation. The applied channel model was the modified Saleh-Valenzuela model 1 [6].

For simplicity, 128 sub-carriers are utilized for transmission, although in the proposal only 122 are suggested for real

transmission [1]. The number of sub-carriers assigned for pilot estimation can be 16, 32, 64 or 128. In the 128 sub-carrier case, interpolation is not needed. For the 16 and 32 cases, CT arrangement has been adopted, while for the 64 and 128 cases, BT is used. Therefore, the 64 case can be considered as a simplified solution for higher data rate systems, since half of the sub-carriers in the block are available for data transmission.

Figures 3 and 4 show the results for time domain estimation, without and with a Wiener filter, respectively. As one can notice, the use of an additional Wiener filter gives an improvement of around 1 dB only for the 64 sub-carrier case, while in the other cases no relevant improvement is noticed. That is, Wiener filtering has a noticeable effect only for the BT approach. Except for this case, however, we can assume that Wiener filtering can be discarded as an interesting option, due to the increasing receiver complexity.

In the results of Figures 5 and 6, LS estimator is performed with a linear and cubic interpolation, respectively. No significant difference in the performances can be noticed.

Figure 7 shows the results when LMMSE estimator is performed with a cubic interpolation. If compared to the LS estimator, the performance is increased only for low  $E_b/N_0$  values. This similar behavior is typical for uncoded systems [5]. The only exception is the 16 sub-carrier case, in which LMMSE has a poorer performance than in LS.

Finally, Figure 8 shows the effects of phase compensation for both LS and LMMSE approach. As one can notice, there is a performance improvement of around 2 dB for the 32 sub-carrier case. That is in CT arrangement, where frame synchronisation is a critical issue and phase compensation is required when a low number of sub-carriers is used (16 and 32). Otherwise, no changes are noticed in the case of BT arrangement. The use of LMMSE could be avoided, since it requires knowledge of the autocorrelation of the channel impulse response.

Comparing time and frequency based algorithms, we could claim that frequency based methods give better results than time based methods for most of the used pilot sub-carrier sets (32, 64, 128). The improvement is in order of 2 – 4 dB.

#### IV CONCLUSIONS AND FURTHER DEVELOPMENT

In this paper, we have studied the effects of channel estimation in ultra wideband (UWB) systems using a multiband-OFDM (MB-OFDM) approach. Several time and frequency channel estimation algorithms have been considered. In addition, phase compensation has been taken into account.

Results showed that in time domain estimation, the use of an additional Wiener filter gives an improvement of around 1 dB only for the 64 sub-carriers case, thus being not suitable for a low-complexity implementation. In frequency domain estimation, the use of a LS estimator shows similar performance with linear and cubic interpolation. Same results are obtained for the LMMSE case, which compared to the LS estimator, gives better performance only for low  $E_b/N_0$  values. Thus, the use of an LS estimator with linear interpolation appears to be the best choice. This behavior is typical for uncoded systems. Frequency based methods give an improvement of 2 – 4 dB if compared to the time based ones for most of the used pilot sub-carrier sets (32, 64, 128).

If phase compensation is adopted, a performance improvement of around 2 dB is noticed for the 32 sub-carriers case in both LS and LMMSE case, leading us to claim that phase compensation is required in comb-type arrangements only when a low number of pilot sub-carriers is used (16, 32). In this case, the use of the LS approach is suggested, since it does not require the knowledge of the autocorrelation matrix of the channel.

As a further development of the research concerning TD algorithms, a comparison of the proposed methods with the ones presented in [14] may be attempted, where a different weighting approach than the one in (13) is used, leading to a "low complexity" implementation. In particular, it can be interesting to compare it with the linear and cubic interpolation in terms of benefit and cost. Moreover, for the comb-type pilot arrangement, the possible benefits of a sliding pilot arrangement could be inspected, in order to see the possible help this could give in case the pilot signals are caught in low SNR sub-carriers.

#### V ACKNOWLEDGMENT

This study has been financed by the Finnish Academy (CAMU, decision number 107592), and the Finnish Funding Agency for Technology and Innovation (Tekes), Elektrobitt and the Finnish Defence Forces through CUBS project. The authors would like to thank all the sponsors for their support and Chalmers University of Technology, Sweden, for co-operation in the multiband-OFDM simulator development.

#### VI REFERENCES

- [1] A. Batra et al. *Multi-band OFDM Physical Layer Proposal for IEEE 802.15 Task Group 3a*. Doc.: IEEE P802.15-03/268r2, 2003.
- [2] G. Shor. *TG3a-Wisair-CFP-Presentation*. Doc.: IEEE 802.15-03/151r3.
- [3] G.R. Aiello and G.D. Rogerson. *Ultra-Wideband Wireless Systems*. *IEEE Microw. Mag.*, 4(2): 36-47, June 2003.
- [4] R.A. Cepeda. *Spectral Analysis and Correlation Properties of MultiBand UWB Pulses*. In *Proc. Ultra Wide Band Summit*, 2003.
- [5] J. Heiskala and J. Terry. *OFDM Wireless LANs: A Theoretical and Practical Guide*. Sams Publishing 2002.
- [6] J. Foerster et al. *Channel modeling sub-committee report final*. IEEE P802.15 Wireless Personal Area Networks, P802.15-02/490r1-SG3a, 2003.
- [7] B. Mielczarek, M.-O. Wessman and A. Svensson. *Performance of Coherent UWB Rake Receivers using different Channel Estimators*. In *Proc. 2003 Int'l Workshop on Ultra Wideband Systems*, 2003.
- [8] M.-O. Wessman, A. Svensson and E. Agrell. *Frequency Diversity Performance of Coded Multiband-OFDM Systems on IEEE UWB Channels*. In *Proc. IEEE VTC-Fall*, 2004.
- [9] O.-S. Shin, S.S. Ghassemzadeh, L.J. Greenstein and V. Tarokh. *Performance Evaluation of MB-OFDM and DS-UWB Systems for Wireless Personal Area Networks*. In *Proc. IEEE 2005 Int'l Conference on Ultra Wideband*, pages 214 – 219, 2005.
- [10] J. K. Cavers. *An Analysis of Pilot Symbol Assisted Modulation for Rayleigh Fading Channels*. *IEEE Trans. Signal Process.*, 49: 3065-3073, December 2001.
- [11] M.-H. Hsieh and C.-H. Wei. *Channel Estimation for OFDM Systems Based on Comb-Type Pilot Arrangement in Frequency Selective Fading Channels*. *IEEE Trans. Consum. Electron.*, 44(1): 217-225, February 1998.
- [12] G. Auer, S. Sand and A. Dammann. *Comparison of low complexity OFDM channel estimation techniques*. In *Proc. 8<sup>th</sup> Int'l OFDM Workshop*, pages 157-161, 2003.
- [13] O. Edfors, M. Sandell, J.-J. van de Beek, S.K. Wilson and P.O. Börjesson. *OFDM Channel Estimation by Singular Value Decomposition*. *IEEE Trans. Commun.*, 46(7): 931-939, July 1998.
- [14] L. Deneire, P. Vandenameele, L. van der Perre, B. Gyselinckx and M. Engels. *A Low-Complexity ML Channel Estimator for OFDM*. *IEEE Trans. Commun.*, 51(2): 135-139, February 2003.

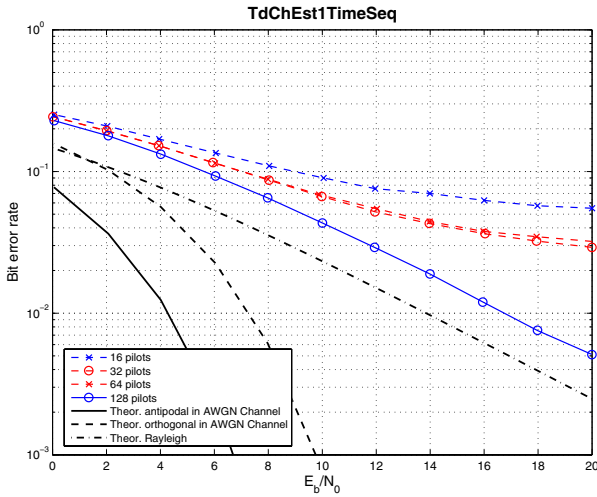


Figure 3. BER vs. SNR for TD channel estimation for different number of sub-carriers.

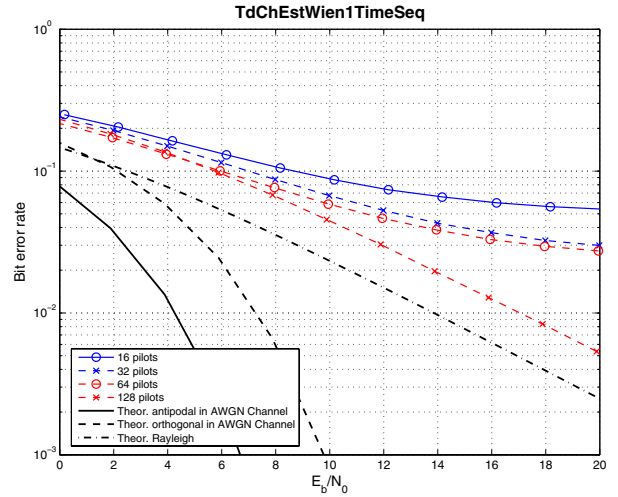


Figure 4. BER vs. SNR for TD channel estimation with Wiener filtering for different number of sub-carriers.

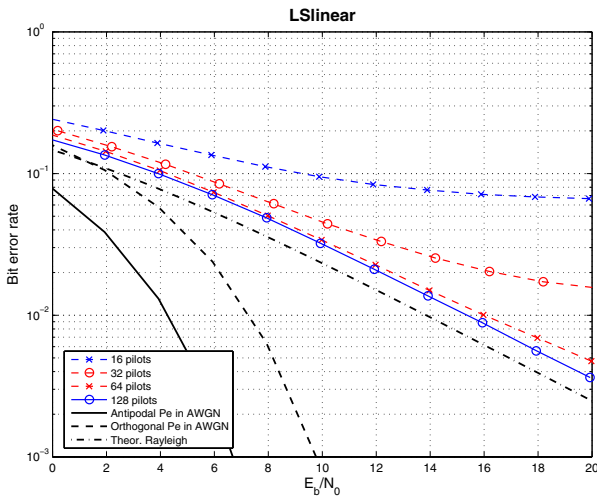


Figure 5. BER vs. SNR for LS estimation for different number of sub-carriers with linear interpolation.

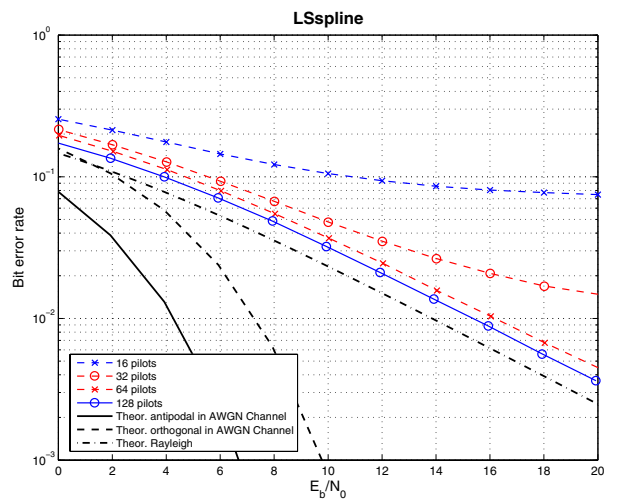


Figure 6. BER vs. SNR for TD channel estimation for different number of sub-carriers with cubic interpolation.

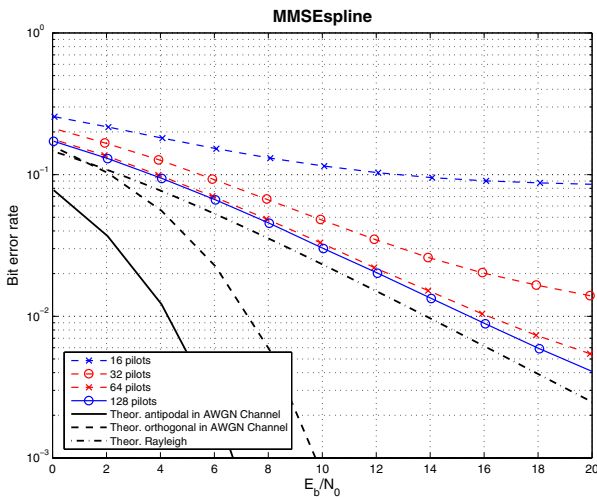


Figure 7. BER vs. SNR for LMMSE estimation for different number of sub-carriers with cubic interpolation.

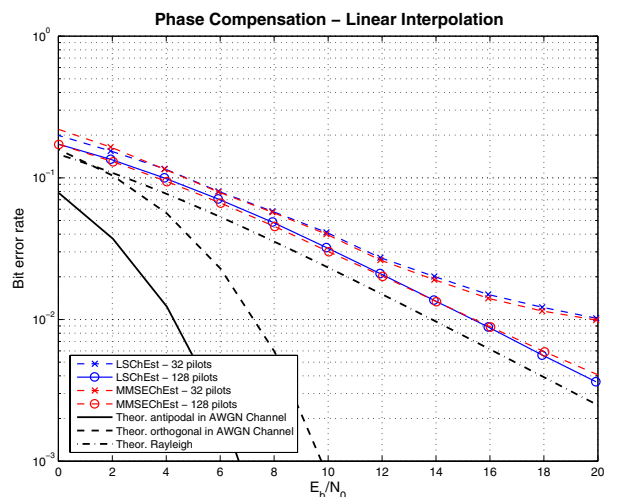


Figure 8. BER vs. SNR for LS and LMMSE estimation for different number of sub-carriers with linear interpolation and phase compensation.